

# ACTIVE SUPPRESSION OF MICROPHONICS DETUNING IN HIGH $Q_L$ CAVITIES\*

N. Banerjee<sup>†</sup>, G. Hoffstaetter, M. Liepe, P. Quigley

Cornell Laboratory for Accelerator-Based Sciences and Education, Ithaca, USA

## Abstract

Accelerators operating with low beam loading such as Energy Recovery Linacs (ERL) greatly benefit from using SRF cavities operated at high loaded quality factors, since it leads to lower RF power requirements. However, large microphonics detuning several times the operating bandwidth of the cavities severely limit the maximum accelerating fields which can be sustained in a stable manner. In this talk, I will describe an active microphonics control technique based on the narrow band Active noise Control (ANC) algorithm which we have used in CBETA, a multi-turn SRF ERL being commissioned at Cornell University. I will describe its stability and performance during beam operations of CBETA with consistent reduction of peak detuning by almost a factor of 2 on multiple cavities.

## INTRODUCTION

Superconducting Radio Frequency (SRF) technology is continuously pushing the boundaries of maximum gradients and thermal efficiency allowing us to operate CW Linacs with lower cryogenic requirements. At the same time, there is also a push towards high loaded quality factors  $Q_L \approx 10^8$  for linacs operating with low beam loading such as in Energy Recovery Linacs (ERL) (eg. CBETA [1], bERLinPro [2]) and Free Electron Lasers (eg. LCLS-II [3], XFEL [4]). The larger quality factors lead to lower average power requirements making efficient solid state amplifiers an attractive option. However, the smaller bandwidth arising from the large  $Q_L$  makes the system more sensitive to resonance detuning resulting in a trade off between RF power requirements and field stability. In this context, suppression of microphonics detuning is becoming more important for improving the RF power usage of SRF Linacs.

The power required to operate SRF cavities at a fixed frequency with the electric field kept at a constant amplitude and phase with respect to a master clock fluctuates with resonance detuning. Transient changes in the resonance frequency of the cavity resulting from mechanical deformations changes its response to incoming RF waves and results in enhanced reflection at the fundamental power coupler. The RF power  $P$  required to maintain a voltage  $V$  with zero beam loading is given by, [5]

$$P = \frac{V^2}{8 \frac{R}{Q} Q_L} \frac{\beta + 1}{\beta} \left[ 1 + \left( \frac{2Q_L \Delta\omega}{\omega_0} \right)^2 \right], \quad (1)$$

where  $\Delta\omega$  is the detuning,  $R/Q$  is the shunt impedance in circuit definition and  $\beta$  is the coupling factor. Hence, efforts toward suppression of peak detuning in machines operating with high  $Q_L$  starts at the design level by introducing stiffening rings to reduce the sensitivity of the resonance frequency to mechanical perturbations. [6] Identification and suppression of vibration sources is the most important method of reducing peak detuning. In this paper, we discuss using the Active Noise Control (ANC) algorithm as a method of active suppression of microphonics when passive measures are not feasible.

In the next section, we describe the narrow-band Active Noise Control (ANC) algorithm, along with a modification based on the Least Mean Square (LMS) technique. Then we demonstrate its performance in the main linac [7] used for energy recovery at the Cornell-BNL ERL Test Accelerator (CBETA) project. Finally, we present a summary of this work and propose some improvements for the future.

## ACTIVE NOISE CONTROL

Active suppression of microphonics detuning requires fast tuners which respond at acoustic time scales using piezoelectric actuators such as the one used in CBETA which has a range of about 2 kHz or about 100 times the operating bandwidth of the cavity. [8] The dynamic mechanical response of the fast tuner can be described using a Linear Time Invariant (LTI) response model. In the frequency domain, the change in resonance frequency  $\delta\tilde{f}(\omega)$  of the cavity in response to the applied voltage  $\tilde{u}_{pz}(\omega)$  is given by,

$$\delta\tilde{f}(\omega) = \tau(\omega)\tilde{u}_{pz}(\omega), \quad (2)$$

where  $\tau(\omega)$  is the frequency response or transfer function of the tuner. The frequency spectrum of microphonics along with the frequency response of the tuner greatly influences the design of the active resonance control system. The transfer functions measured on three cavities of the main linac in CBETA are shown in Fig. 1. The transfer function measurements show a region of flat amplitude and linear phase response in the range of low frequencies up to 30 Hz; this makes the use of simple algorithms like proportional-integral (PI) control feasible for attenuating low frequency microphonics. If the microphonics spectral lines at higher frequencies are narrow-band and not near any mechanical resonances of the tuner, then the Active Noise Control (ANC) algorithm becomes a very simple and effective method of actively suppressing microphonics detuning.

Microphonics from narrow band vibration sources may be represented by a finite series of sinusoids at different frequencies with slowly changing amplitudes and phases.

\* This work was supported by the New York State Energy Research and Development Authority and NSF award DMR-0807731.

<sup>†</sup> nb522@cornell.edu

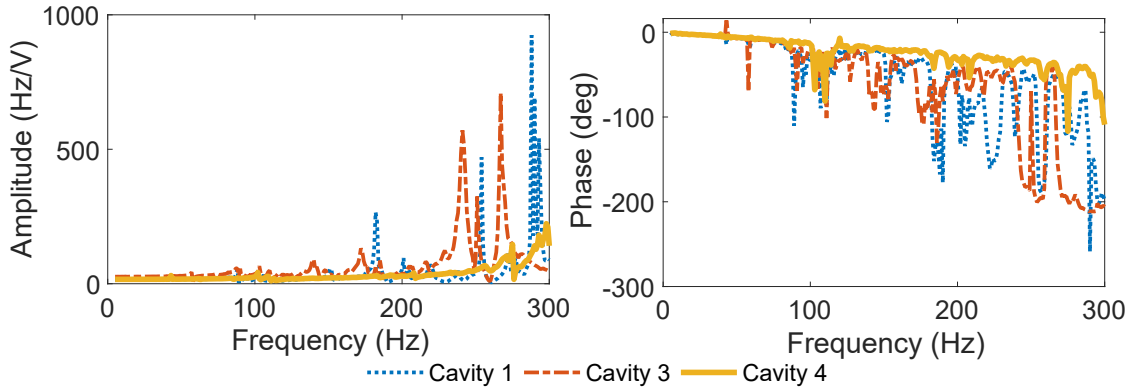


Figure 1: Tuner response amplitude and phase as functions of frequency of applied voltage for three cavities of the main linac used in CBETA. The plots show multiple strong resonances above 200 Hz for unstiffened cavities 1 and 3. Cavity 4 is fitted with stiffening rings which suppress the low frequency eigenmodes of the structure.

Hence, in the time domain, the actuator voltage  $u_{pz}(t)$  can be written as a sum of sinusoids  $u_m(t)$  with frequencies  $\omega_m$  and whose amplitudes and phases are determined by slowly changing phasors  $\tilde{A}_m(t)$  using the relation,

$$u_{pz}(t) = \sum_m u_m(t) = \sum_m \text{Re}\{\tilde{A}_m(t)e^{i\omega_m t}\}. \quad (3)$$

In order to calculate the dynamic response of the resonance frequency of the cavity in a narrow domain, we can approximate the transfer function of the tuner as a constant  $\lim_{\omega \rightarrow \omega_m} \tau(\omega) = \tau_m^{\text{mod}} e^{-i\phi_m^{\text{mod}}}$ . The effective resonance frequency of the cavity  $\delta f_{\text{comp}}(t)$  under external vibrations  $\delta f_{\text{ext}}(t)$  and actuation of the tuner is given by, [9]

$$\delta f_{\text{comp}}(t) = \delta f_{\text{ext}}(t) + \sum_m \text{Re}\{\tau_m^{\text{mod}} \tilde{A}_m(t) e^{i(\omega_m t - \phi_m^{\text{mod}})}\} \quad (4)$$

We can use this model of compensated detuning to construct the ANC algorithm.

The technique of narrow-band ANC, demonstrated in the past as an effective resonance control algorithm [10, 11], may be derived in a Least Mean Square (LMS) sense as a stochastic gradient descent minimization [12] of the cost function,

$$C(t_n) = [\delta f_{\text{comp}}(t_n)]^2, \quad (5)$$

where  $C(t_n)$  is the expectation value of the square of detuning. Each iteration of gradient descent changes the actuation phasors  $\tilde{A}_m(t)$  a little in a direction opposite to the gradient using the relation,

$$\tilde{A}_m(t_{n+1}) = \tilde{A}_m(t_n) - \mu_m \delta f_{\text{comp}}(t_n) e^{i(\omega_m t - \phi_m^{\text{mod}})}, \quad (6)$$

where  $\mu_m$  is learning rate of the algorithm. Equation (3) together with Eq. (6) form the narrow-band ANC algorithm.

The ANC algorithm described here is mathematically equivalent to applying a linear filter on the tuning error  $e(t) \equiv -\delta f_{\text{comp}}(t)$ , whose Z transform can be written as,

$$H_m(z) = \mu_m \frac{\cos(\omega_m \Delta t + \phi_m^{\text{mod}}) - z^{-1} \cos \phi_m^{\text{mod}}}{1 - 2 \cos(\omega_m \Delta t) z^{-1} + z^{-2}}, \quad (7)$$

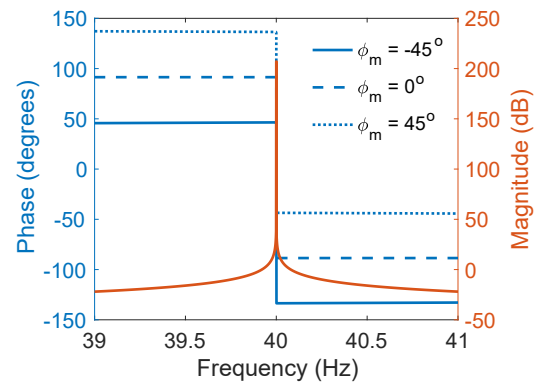


Figure 2: Frequency response  $H_m(e^{i\omega t})$  of the control filter described in Eq. (7) for one mode  $f_m = 40$  Hz,  $\mu_m = 10^{-4}$ ,  $\Delta t = 0.1$  ms and three values of phase  $\phi_m = -45^\circ, 0^\circ, 45^\circ$ . The value of  $\phi_m$  primarily provides a constant offset to the phase response and can be used as a knob to stabilize the feedback control loop.

where  $\Delta t$  is the time between each iteration. The frequency response of this filter shown in Fig. 2 has a very narrow bandpass behavior with the amplitude rising to  $\infty$  and a phase swing of  $180^\circ$  around the frequency  $\omega_m$ . While the gain  $\mu_m$  controls the width of the peak, the phase  $\phi_m^{\text{mod}}$  should ideally match the phase response of the tuner. In reality, the actual phase response of the tuner  $\phi_m^{\text{mod}}$  might be different from the phase  $\phi_m$  used during compensation, and hence analyzing the stability of the ANC algorithm is important.

The complete stability analysis of the ANC system involves assessing the open loop transfer function  $\mathcal{U}_m(\omega) \equiv \tau(\omega) \sum_m H_m(\omega)$  over all frequencies using a Bode plot. Figure 3 shows an example of using the compensation system on an unstiffened cavity used in the main linac of the CBETA project. We apply the algorithm on two frequencies 8 Hz

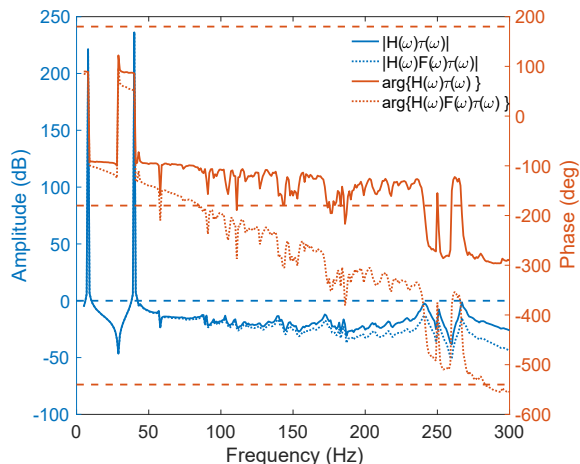


Figure 3: Bode plot for the mechanical open loop transfer function  $\mathcal{U}(\omega) \equiv H(\omega)\tau(\omega)$  of an unstiffened cavity inside the main linac used for the CBETA project, showing both the amplitude and phase in blue and orange respectively. The solid lines represent the effect of the ANC algorithm applied to frequencies 8 Hz and 40 Hz, while the dotted lines represent the effect of incorporating a low pass filter with frequency response  $F(\omega)$  inside the controller. The blue dashed line represents unity gain (0 dB) and the orange dashed lines at  $-540^\circ$ ,  $-180^\circ$  and  $180^\circ$  represents the boundaries of stability in phase.

and 40 Hz illustrated by the notches in amplitude and expected phase swings of  $180^\circ$  at these frequencies. The open loop phase stays between the  $-180^\circ$  and  $180^\circ$  lines for gains above 0 dB showing that the system is stable near these frequencies. The phase margins i.e the distances from the  $-180^\circ$  line when the amplitude crosses unity gain (0 dB) are  $80^\circ$  and  $90^\circ$  at 8 Hz and 40 Hz respectively as seen from the plot of  $\phi_{OL} = \arg\{H(\omega)\tau(\omega)\}$  in Fig. 3. However, the gain seems to be close to 0 dB near the tuner resonances at frequencies around 250 Hz, when  $\phi_{OL}$  crosses the  $-180^\circ$  mark with a gain margin  $\lesssim 2$  dB. This prompts the use of a low pass filter with frequency response  $F(\omega)$  to attenuate the transfer function at these frequencies as shown by the dotted lines of Fig. 3. The analysis illustrates the effect of tuner resonances far from the compensation frequencies  $\omega_m$  signalling the need for additional filtering to ensure stability of the system.

The compensation performance of a controller with fixed parameters is dependent on variations in the response of the tuner and fluctuations of the microphonics spectrum. The tuner response may vary from day to day due to pressure variation in the Helium bath while the vibration mechanism may also change frequency as a function of time. The ANC controller will not be able to adapt to such changes, which might limit performance in a dynamic environment. We derive a modification to the algorithm which adapts the controller phase  $\phi_m$  in order to minimize the cost function

through gradient descent, and in this way make the controller more robust to changes in the tuner. The partial derivative of the cost function given in Eq. (5) with respect to  $\phi_m$  is given by,

$$\frac{\partial C}{\partial \phi_m} = 2\tau_m \delta f_{\text{comp}}(t_n) \text{Re}\{\tilde{A}_m(t_n) e^{i(\omega_m t_n - \phi_m(t_n) - \pi/2)}\}. \quad (8)$$

This gives us the update rule

$$\phi_m(t_{n+1}) = \phi_m(t_n) - \eta_m \delta f_{\text{comp}}(t_n) \times \text{Re}\{\tilde{A}_m(t_n) e^{i(\omega_m t_n - \phi_m(t_n) - \pi/2)}\}, \quad (9)$$

where  $\eta_m$  is the adaptation rate for  $\phi_m$ . This modification is used in our implementation of the ANC algorithm to achieve consistent performance with minimal effort.

## PERFORMANCE

We have used the modified ANC algorithm during various stages of RF commissioning to attenuate microphonics and the results from un-stiffened cavities of the main linac are shown in Fig. 4. The first two panels show the performance when we applied the compensation for 41 Hz and 8 Hz on un-stiffened cavities 1 and 3. The algorithm was successful in attenuating 41 Hz in both cavities 1 and 3 but was not effective on 8 Hz vibrations in cavity 3 as illustrated by the spectrum plots probably because the compensation frequency was not set precisely. These narrow band vibrations were a major contribution to microphonics detuning and their decrease also reduced the peak detuning. After a warm-up cool-down cycle, we found the major source of microphonics detuning to be at 59 Hz. The ANC algorithm was successful in suppressing these vibrations in cavity 3. The attenuation of spectral lines are further validated by the RMS detuning as listed in Table 1. The success of the algorithm indicates that those vibration lines were not in the vicinity of mechanical eigen modes of the tuner-cavity system. The results of using the system on stiffened cavities 4 and 6 at the frequencies 8 Hz and 41 Hz with additional attenuation of 82 Hz on cavity 6 is shown in Fig. 5. While the ANC successfully reduced peak detuning from 30 Hz to 15 Hz in cavity 6, the measurements on cavity 4 indicate no reduction of peak detuning even though the RMS detuning is attenuated as seen from both the histogram and the spectrum plot. In all cavities, we observe additional spectral lines generated by the ANC controller which correspond to transients arising from the non-linear phase adaptation process. Nevertheless, the ANC algorithm is well suited for compensating narrow band vibrations in both stiffened and un-stiffened cavities as evidenced from the performance listed in Table 1.

The stability and robustness of the algorithm is demonstrated by comparatively long periods of stable operation with the same settings on different days. The observations shown in Table 1 are taken from data sets of at least 800 seconds measured for cavities inside a cryomodule connected to a production level cryogenic system unlike previous work

Content from this work may be used under the terms of the CC BY 3.0 licence (© 2019). Any distribution of this work must maintain attribution to the author(s), title of the work, publisher, and DOI.

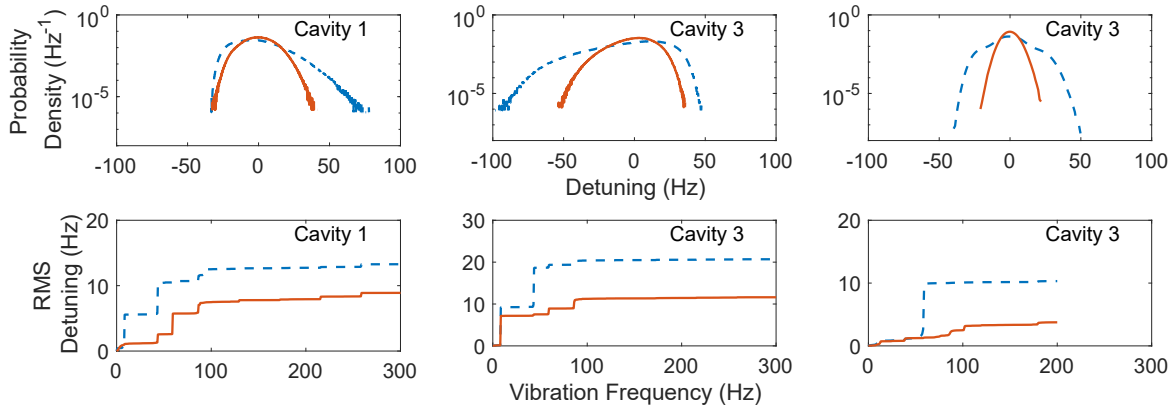


Figure 4: Microphonics measurements showing illustrating the performance of the modified ANC on two un-stiffened cavities of the main linac. The dashed lines represent data without active suppression while the bold lines show the performance with ANC turned on. The third data set was taken after a warm-up cool-down cycle.

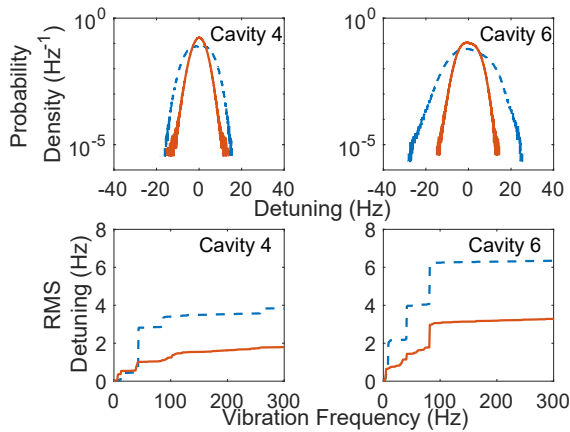


Figure 5: Effect of active microphonics compensation on two stiffened cavities of the main linac. The dashed lines represent data without active suppression while the bold lines show the performance with ANC turned on.

Table 1: Results of Using the Active Noise Control System on Various Cavities During Different Stages of Commissioning. Cavities 1 and 3 are un-stiffened while 4 and 6 have stiffening rings. The two data sets for cavity 3 were taken during two different stages of commissioning.

Cavity	Peak Detuning (Hz)		RMS Detuning (Hz)	
	ANC Off	ANC On	ANC Off	ANC On
1	78	45	13.6	9.1
3	100	57	20.8	11.7
3	50	22	10.7	4.6
4	17	19	4.4	2.4
6	30	15	6.4	3.4

primarily focused on test facilities. We achieved stable operations of over a few hours without spontaneous trips on all cavities with the ANC system active. Throughout the commissioning process we have been successfully using it on various cavities during beam operations for the CBETA. Once the settings are determined using the procedure explained elsewhere [9], resonance control is turn key with no tweaking required on subsequent days of operation which highlights the robustness of the system.

## CONCLUSION

The recent push towards using efficient solid state RF amplifiers have led to more accelerators operating SRF cavities with comparatively high loaded quality factors  $Q_L \approx 10^8$ . While this reduces average power requirements by a significant margin, it also increases sensitivity towards microphonics detuning caused by different mechanical perturbations. Microphonics suppression is thus very important in accelerators such as emerging ERL and FEL projects which operate in this regime. While careful mechanical design of cavities and cryomodules can go a long way towards this goal, the primary method remains characterization and attenuation of vibration sources during the process of cryomodule test and commissioning. Active suppression becomes important for reducing the effects of detuning when such meticulous studies are not feasible. In this paper we describe a modified narrow-band Active Noise Control (ANC) algorithm which can be used for active resonance control to ensure field stability within the RF power constraints.

The method used for active microphonics compensation depends on both the frequency response of the tuner and the microphonics spectrum. When the microphonics spectral lines are sufficiently narrow, we can approximate the required actuator voltage as a sum of sinusoids with slowly varying amplitudes and phases. Further, if the frequency of detuning is far away from mechanical resonances of the

cavity-tuner system, we can approximate the tuner response by a constant value  $\lim_{\omega \rightarrow \omega_m} \tau(\omega) = \tau_m^{\text{mod}} e^{-i\phi_m^{\text{mod}}}$ . Under these assumptions we can derive the ANC algorithm which adjusts the amplitudes and phases of sinusoids at the frequency of microphonics through stochastic gradient descent. The stability of this algorithm depends strongly on the gain  $\mu_m$  and phase  $\phi_m$  used in Eq. (6) along with the complete frequency response of the tuner. In order to make the algorithm more robust towards changes in tuner response, we derived a modification which adapts the phase  $\phi_m$  to minimize mean square detuning. The microphonics detuning measured in the main linac used in the CBETA project closely match the requirements of the modified ANC algorithm, making it a perfect candidate for use.

The modified ANC algorithm has been used routinely in various stages of commissioning of CBETA with stable performance during beam operations. The results summarized in Table 1 show consistent reduction of peak detuning by almost a factor of 2 on both stiffened and un-stiffened cavities. The stability and robustness of the algorithm is demonstrated by comparatively long periods of stable operation with the same settings on different days. At the same time, we observe additional spectral lines generated by the ANC controller which correspond to transients arising from the non-linear phase adaptation process. Future work will involve systematic analysis of this effect and automatic configuration of the compensation parameters to make this system completely turn-key.

## ACKNOWLEDGEMENTS

We would like to thank Dan Sabol, Colby Shore and Eric Smith for setting up the cryogenic systems for both cryomodules and help in optimizing the Helium control loops. This work was supported by the New York State Energy Research and Development Authority while the CLASSE facilities are operated with major support from the National Science Foundation. Nilanjan would like to thank the organizing committee of the SRF workshop for providing travel support.

## REFERENCES

- [1] G. H. Hoffstaetter *et al.*, “CBETA, the 4-Turn ERL with SRF and Single Return Loop”, in *Proc. 9th Int. Particle Accelerator Conf. (IPAC'18)*, Vancouver, Canada, Apr.-May 2018, pp. 635–639. doi : 10.18429/JACoW-IPAC2018-TUYGBE2
- [2] M. Abo-Bakr *et al.*, “Status Report of the Berlin Energy Recovery Linac Project BERLinPro”, in *Proc. 9th*

*Int. Particle Accelerator Conf. (IPAC'18)*, Vancouver, Canada, Apr.-May 2018, pp. 4127–4130. doi : 10.18429/JACoW-IPAC2018-THPMF034

- [3] C. Hovater *et al.*, “The LCLS-II LLRF System”, in *Proc. 6th Int. Particle Accelerator Conf. (IPAC'15)*, Richmond, VA, USA, May 2015, pp. 1195–1197. doi : 10.18429/JACoW-IPAC2015-MOPWI021
- [4] J. Branlard *et al.*, “LLRF System Design and Performance for XFEL Cryomodules Continuous Wave Operation”, in *Proc. 16th Int. Conf. RF Superconductivity (SRF'13)*, Paris, France, Sep. 2013, paper THP086, pp. 1129–1131.
- [5] M. Liepe and S. Belomestnykh. “RF Parameter and Field Stability Requirements for the Cornell ERL Prototype”, in *Proc. PAC'03*, Portland, OR, USA, May 2003, paper TPAB056, pp. 1329–1331.
- [6] S. Posen and M. Liepe, “Mechanical optimization of superconducting cavities in continuous wave operation”, *Phys. Rev. ST Accel. Beams*, vol. 15, p. 022002, Feb. 2012.
- [7] F. Furuta *et al.*, “Performance of the Novel Cornell ERL Main Linac Prototype Cryomodule”, in *Proc. 28th Linear Accelerator Conf. (LINAC'16)*, East Lansing, MI, USA, Sep. 2016, pp. 492–495. doi : 10.18429/JACoW-LINAC2016-TUPLR011
- [8] S. Posen and M. Liepe, “Measurement of the Mechanical Properties of Superconducting Cavities During Operation”, in *Proc. 3rd Int. Particle Accelerator Conf. (IPAC'12)*, New Orleans, LA, USA, May 2012, paper WEPPC081, pp. 2399–2401.
- [9] Banerjee, Nilanjan *et al.*, “Active suppression of microphonics detuning in high  $Q_L$  cavities”, *Phys. Rev. ST Accel. Beams*, vol. 22, p. 052002, 2019.
- [10] T.H. Kandil, H.K. Khalil, J. Vincent, T.L. Grimm, W. Hartung, J. Popielarski, R.C. York, S. Seshagiri, “Adaptive feedforward cancellation of sinusoidal disturbances in superconducting rf cavities”, *Nuclear Instruments and Methods in Physics Research Section A: Accelerators, Spectrometers, Detectors and Associated Equipment*, vol. 550, no. 3, pp. 514–520, 2005.
- [11] R. Rybaniec, K. Przygoda, W. Cichalewski, V. Ayvazyan, J. Branlard, Ł. Butkowski, S. Pfeiffer, C. Schmidt, H. Schlarb, and J. Sekutowicz, “FPGA-based rf and piezocontrollers for srf cavities in cw mode”, *IEEE Transactions on Nuclear Science*, vol. 64, no. 6, pp. 1382–1388, June 2017.
- [12] S. M. Kuo and D. R. Morgan, “Active noise control: a tutorial review”, *Proceedings of the IEEE*, vol. 87, no. 6, pp. 943–973, Jun. 1999.